The influence of different concrete additions on the properties of lightweight concrete evaluated using experimental and numerical approaches

Sang-Yeop Chung[†], Mohamed Abd Elrahman[†,‡,*], Dietmar Stephan[†], Paul H. Kamm[§]

[†] *Building Materials and Construction Chemistry, Technische Universität Berlin,*
Gustav-Meyer-Allee 25, 13355 Berlin, Germany
[‡] *Structural Engineering Department, Mansoura University,*
Elgomhouria St., Mansoura City 35516, Egypt
[§] *Institute of Applied Materials, Helmholtz Centre Berlin,*
Hahn-Meitner-Platz 1, 14109 Berlin, Germany

August 24, 2018

Abstract

Lightweight concrete is a building material used for better insulation and lower energy consumption. The material properties of lightweight concrete, such as compressive strength and thermal conductivity, are strongly affected by the characteristics of its aggregate, binder, and other concrete additions. This study aims to investigate the effects of different concrete additions on the performance of lightweight concrete. Six different materials were used as concrete additions: limestone powder, expanded clay (Liapor®), fine fly ash, fly ash, and fine and normal sand. For lightweight concrete specimens, expanded glass granulate, i.e., Liaver®, was used as a lightweight aggregate to clarify the effects of concrete addition type, with all specimens designed so as to have a density between 800 to 950 kg/m^3. The effects of different concrete additions on the characteristics and properties of lightweight concrete were investigated using several approaches; X-ray micro-computed tomography (μ-CT) was adopted to examine microstructural characteristics, with both the mechanical and thermal properties of the materials being measured using experimental tools. Numerical analysis was also conducted to validate the performance of the materials. The results show that supplementary materials can improve the performance of lightweight concrete with regard to both compressive strength and thermal conductivity.

Keywords: lightweight concrete, concrete addition, filler, μ-CT, compressive strength, thermal conductivity

*Corresponding author. Tel.: +49-30-314-72-104, Fax.:+49-30-314-72-110, E-mail: mohattia76@gmail.com (M. Abd Elrahman)

1 Introduction

Concrete is the most widely used construction materials in the world. There are several types of concrete in use, including structural lightweight concrete, shrinkage-compensating concrete, and heavyweight concrete for radiation shielding [1, 2]. Lightweight concrete is widely used as a supplementary building material due to its low density and effective insulation [3, 4, 5, 6]. Since environmental matters, such as the recycling of industrial waste and enhancing energy efficiency, have become worldwide issues, sustainable development is desirable in engineering fields, including construction industry. For this purpose, many efforts to reduce energy consumption and save energy in the construction industry and building material field have been undertaken in recent years; lightweight concrete is considered to be one of the most important building materials which can contribute to the development of sustainable materials.

In general, lightweight concrete is produced by using natural or artificial lightweight aggregates instead of normal aggregates. Various materials have been studied and used as lightweight aggregates in developing advanced lightweight concrete with better material properties. For instance, expanded clay [7] or recycled materials, such as expanded glass [8], masonry rubble [9], and crushed glass [10], have been used as lightweight aggregates, and concrete materials with these lightweight aggregates have shown better insulation performance than conventional concrete. Lightweight aggregates generally occupy more than 50% of the concrete volume; therefore, it is important to use appropriate aggregates to achieve the target performance of concrete materials [11, 12, 13, 14].

However, although the rest of the concrete volume is filled with a binder (or matrix) material, relatively less attention has been paid to the binder of lightweight concrete, despite its importance. For concrete binder, ordinary Portland cement (OPC) is the most common and essential material, with more than 4.2 billion tons of OPC being consumed annually in the construction industry; therefore, OPC is an essential element in lightweight concrete. Nevertheless, it is well known that the production of cement is considered to be one of the major sources of CO_2 emissions, and a huge amount of energy is needed to produce OPC, in comparison to the other fundamental components of concrete [15, 16]. To reduce the disadvantages of using cement, the use of supplementary cementitious materials (SCM) as concrete addition is considered to be a promising approach, and several studies have been conducted in relation to the SCMs of lightweight concrete. Zhang et al. [17] investigated the sulfate attack resistance of concrete with different binders by using ground granulated blast furnace slag (GGBS), and Diquelou et al. [18] used hemp and lime as a binder to enhance the mechanical performance of lightweight concrete. Real and Bogas [19] evaluated the oxygen permeability of lightweight concrete with fly ash, silica fume, and lime filler, and Real et al. [20] also performed the chloride migration test of lightweight concrete with different binders. Yu et al. [13] used polypropylene fibers to enhance the material properties of lightweight concrete, and Fu et al. [21] demonstrated the effects of different binders using epoxy

for porous concrete. Shafigh et al. [22] examined the engineering properties of lightweight aggregates containing limestone powder as well as fly ash and found that the use of limestone powder can improve the compressive strength of lightweight concrete. In particular, Mo et al. [23] and Farahani et al. [24] investigated and summarized the effect of different binder materials on concrete properties. Most of these studies were concerned only with lightweight concrete with a density above 1600 kg/m^3, which is a relatively high density for structural lightweight concrete based on the European standard (EN) [25].

The main objective of this study is to produce and investigate the effects of concrete fillers on the performance of lightweight concrete with a low density. According to EN 206-1 [25], lightweight concrete for use as a structural component should have a density between 800 and 2000 kg/m^3. Here, lightweight concrete specimens with a density less than 1000 kg/m^3 were produced, thus satisfying the standards of structural lightweight concrete. To investigate the effects of filler type on the performance of lightweight concrete, the following supplementary materials were used and compared: limestone powder, Liapor$^®$ sand, fine fly ash, fly ash, and fine sand. A lightweight concrete sample with normal sand was also produced as a reference. In all cases, an expanded glass granulate, Liaver$^®$, was used as a lightweight aggregate, only to compare the filler effect on lightweight concrete; the volume of lightweight aggregates was equally fixed in all specimens. Lightweight concrete is generally used for both structural and insulation purposes, and appropriate mechanical and thermal properties are required for the material. Here, the compressive strength and thermal conductivity of the lightweight concrete specimens with different additions were measured using Toni Technik (Germany) and Hot Disk (Sweden) devices, which satisfy European [26] and ISO [27] standards, respectively. The microstructures of the specimens were visualized using micro-level computed tomography (μ-CT). In addition, virtual specimens with the same mix proportions as the real lightweight concrete specimens were generated, and their numerical properties were evaluated using finite element (FE) analysis and compared with the experimental results. With the obtained results, the effectiveness of each supplementary material is discussed, and the proper material is proposed in accordance with the purpose of use.

2 Lightweight concrete specimens with different materials

2.1 Materials

In this study, several concrete mixes with different compositions were prepared and tested. The used cement was CEM III A 42.5 N complying with EN 197-1 which was provided by HeidelbergCement (Germany). Condensed silica fume, provided by Sika Germany which satisfies EN 13263-1, was used to enhance the fresh and the hardened properties of lightweight concrete. To investigate the effects of different additions, several materials, such as limestone powder (sh

Table 1: Physical properties of the used binders and concrete additions

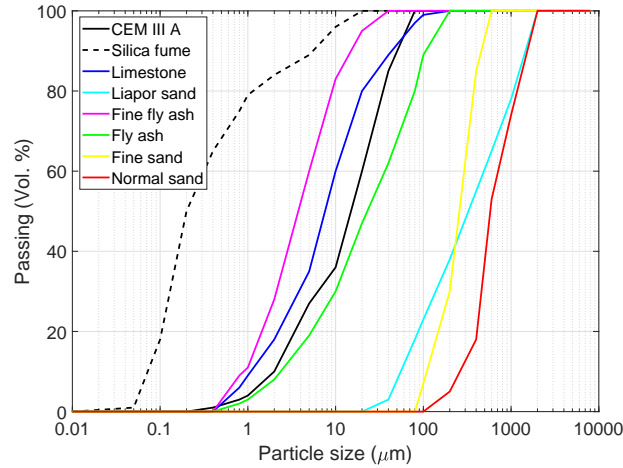| Material	CEM III A	Silica fume	Limestone powder	Liapor® sand	Fine fly ash	Fly ash	Fine sand	Normal sand
Blaine [cm^2/g]	4180	200000	3450	-	6000	3623	760	-
Density [kg/m^3]	3050	2200	2720	1770	2450	2377	2670	2630

Figure 1: Particle size distributions of the materials

minerals, Germany), fine fly ash (Baumineral, Germany), class C fly ash, and fine quartz sand (Sand-schulz, Germany), were used for the specimens. In addition, normal sand and lightweight expanded clay (Liapor® sand) were used to compare their performance with other materials. Table 1 presents the physical properties of the used materials, and their particle size distribution is shown in Fig. 1.

To compare the effects of different concrete additions, other conditions besides the concrete additions need to be fixed. For this purpose, Liaver®-expanded glass-was utilized as a lightweight aggregate for all specimens. Liaver® is made of recycled glass, and its granules are sintered in a rotary kiln between 750 and 900 °C [28]. This material has an almost round shape and a smooth surface with numerous closed pores included in the material. Liaver® was used as a coarse aggregate with three different fractions: 0.5-1.0, 1.0-2.0, and 2-4 mm. The measured properties of the used aggregate are presented in Table 2. In this table, the crushing resistance of the material was provided by the

Table 2: Physical properties of Liaver® aggregates

Aggregate class	Shape	Crushing resistance* [N/mm^2]	Particle density [kg/m^3]	Water absorption 1 hour [wt.%]	Water absorption 24 hours [wt.%]
Liaver® 0.5-1 mm	Rounded	≥ 2.9	450	9	15.4
Liaver® 1-2 mm	Rounded	≥ 2.4	350	10.3	15.8
Liaver® 2-4 mm	Rounded	≥ 2.2	310	8.9	14.4

*the material property is given by the manufacturer

Table 3: Mix composition of LWC specimens [kg/m^3]

Material	LS	LP	FFA	FA	FS	NS
Cement	432					
Silica fume	48					
Superplasticizer	4.8					
Stabilizer (Tylose)	0.66					
Water	206	206	206	206	206	206
Limestone powder	155	-	-	-	-	-
Liapor sand®	-	96	-	-	-	-
Fine fly ash	-	-	140	-	-	-
Fly ash	-	-	-	131	-	-
Fine sand	-	-	-	-	150	-
Normal sand	-	-	-	-	-	150
Liaver® 2-4 mm	47.7					
Liaver® 1-2 mm	46.0					
Liaver® 0.5-1 mm	67.1					

manufacturer, while the other properties, such as particle density and water absorption, were measured according to EN 1097-6 [29]; the data in the table was also adopted for the numerical simulation presented in Section 3.

2.2   Design method of the specimens

This study focused on producing lightweight concrete with a density range between 800 and 1000 kg/m^3, which is the lowest dry density (D1,0) lightweight concrete which can be used in structural elements according to EN 206. The mix design and the grading of aggregate fractions were adopted from [30, 31]. Six different mixes of lightweight concrete were manufactured and tested. All mixes had the same composition, and the only difference is the addition type. The volumetric content of the concrete addition was kept constant (57 l/m^3), and the material type was changed only to evaluate its influence on the concrete properties. Table 3 shows the detailed mix composition of all the mixes. The lightweight concrete specimens with different additions (binders) are denoted here as follows: limestone powder mix (LS), Liapor® mix (LP), fine fly ash mix (FFA), fly ash mix (FA), fine sand mix (FS), and normal sand mix (NS). The water/binder was set to 0.4 for all the mixes, and only the cement and silica fume contents were taken into account when calculating the water content. All mixes had a planned consistency class of F4 according to EN 206-1. To achieve this consistency, an ether-based polycarboxylic superplasticizer, provided by Sika Germany (Sika Viscocrete 1051) with a density of 1.04 g/cm^3, was used. One of the main problems of producing lightweight concrete with a low density is the possible segregation resulting from the large difference between the density of lightweight aggregates and cement paste. To avoid this problem, a viscosity modifying admixture provided by Sika was used (Sika stabilizer, type 10160317). The water absorption of lightweight aggregate is also a significant factor which needs to be considered in relation to mix proportions. As can be seen in Table 2, the water absorption of lightweight concrete

is about 15 % (wt.), which is much higher than that of normal aggregates and can affect workability significantly. In general, two different mixing methods are used for taking into account the water absorption of lightweight aggregate: either presoaking of aggregate for a certain period or adding an equal amount of absorbed water to the mixer. In this study, an amount of water, which equals the absorbed water by aggregates in one hour, was added to the mixer with the original mixing water.

2.3   Preparation of lightweight concrete specimens

To produce the lightweight concrete, a mixer with a capacity of 60 liters was used to mix the concrete. All mixes were prepared with the same mixing procedure. First, the aggregates and the binder materials were mixed in the mixer for one minute. Water was then added, and stabilizer and superplasticizer were adjusted to achieve the required consistency without segregation or bleeding. After measuring the consistency, cubical molds $100 \times 100 \times 100$ mm^3 were filled with concrete and stored in controlled conditions at a temperature of 21 °C and a humidity of 95 %. The samples were demolded after 24 hours and cured under water until the testing day. Several tests, including compressive strength, dry density as well as thermal conductivity, were carried out with these specimens. In addition, μ-CT was used to evaluate the pore characteristic of different lightweight concrete specimens.

3   Characterization and property analysis

Pore characteristics are dominant in the mechanical and thermal properties of lightweight concrete (LWC). Consequently, the porosity and spatial distribution of pores in the microstructure of LWC needed to be investigated in detail. Here, the porosities in the aggregates and different binders of each LWC specimen were investigated using X-ray micro-computed tomography (μ-CT) without damaging the specimens. The uniaxial compressive strength and thermal conductivity of each binder case were also evaluated experimentally and numerically.

3.1   X-ray CT imaging for evaluating material characteristics

In general, concrete has a complex inner structure due to its heterogeneity. However, it is difficult to identify the microstructure of concrete without disturbing the specimen. To overcome this limitation, the microstructures of LWC were obtained using μ-CT for the purposes of characterization. Fig. 2 shows an example of μ-CT image processing. In this figure, μ-CT in 2D is an 8-bit cross-sectional image of a FA (fly ash filler) specimen; this original μ-CT image is expressed by 256 values in a range between 0 (black) and 255 (white), determined by the relative density of the constituents of the material. Each image is composed of 1000×1000 pixels with a pixel size of 29.7 μm. For
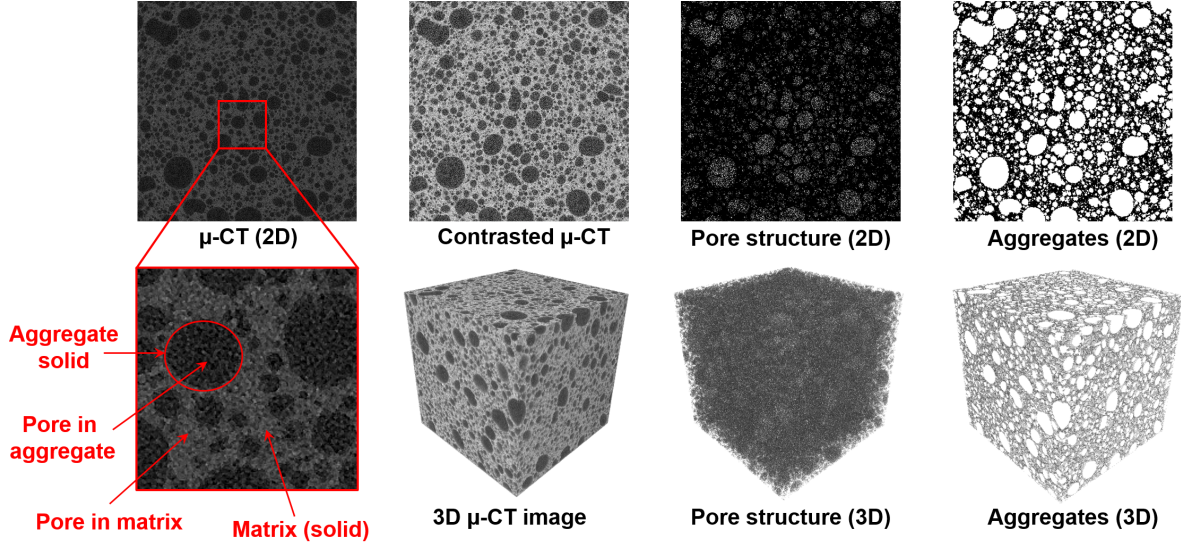
Figure 2: Example of μ-CT image processing to classify pores, aggregates, and binder from FA specimen

instance, in the 8-bit μ-CT image, pores are described in black, and the concrete matrix having the highest density in the specimen is described in light gray. In the other phase, the solid parts of lightweight aggregates are expressed in dark gray, as shown in the figure with the red box; this denotes that the matrix is denser than the solid phases of the lightweight aggregates assuming a comparable material attenuation coefficient. An contrast adjustment was adopted to enhance the image contrast for more effective segmentation of different phases in the specimen. Image segmentation proceeded by use of a multi-level thresholding algorithm based on the grayscale histogram [32]. In this study, the μ-CT images were classified into four categories: matrix, pores within the matrix, aggregate solids, and pores within the aggregates. To describe each aggregate particle of the specimen, a modified watershed model [33] was also adopted for the images. 3D images of the specimen were then obtained by stacking 2D images along a specific (z) direction. The material characteristics, such as porosity, were examined using the obtained 3D microstructures of the specimens with different binders.

3.2 Experimental approaches

The material properties, such as workability, compressive strength, and thermal conductivity, were experimentally evaluated. Flow table tests were performed according to EN 12350-5 in order to produce LWC specimens with different binders. All samples with different filler materials showed flow values between 570 and 640 mm, which can be considered the stable range. The dry density values of the specimens were measured at the age of 28 days after oven drying at 105 °C until constant mass according to EN 12390-7.
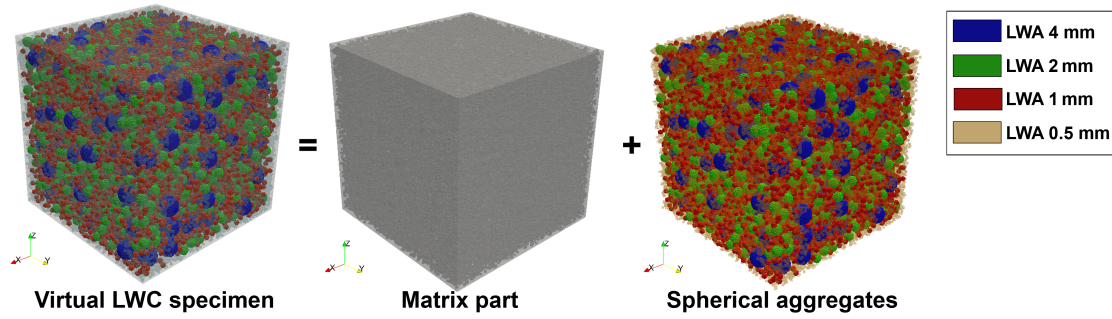
7

Figure 3: Examples of virtual samples with different aggregates (Note: each color represents different aggregate sizes.)

Table 4: The input material properties of different LWAs and binders

Material	Elastic modulus [GPa]	Yield strength [MPa]	Thermal conductivity [W/m/K]	Density [kg/m^3]	Specific heat [J/kg/K]
LWA 0.5 mm	0.83	3.2	0.08	470	1100
LWA 1 mm	0.8	2.9	0.075	380	1140
LWA 2 mm	0.79	2.4	0.073	350	1150
LWA 4 mm	0.45	2.2	0.07	310	1200
LS	33.24	62.50	0.4748	1304	1546
LP	24.23	50.36	0.3643	1100	1253
FFA	33.46	66.07	0.5623	1282	1564
FA	32.14	64.53	0.5242	1253	1522
FS	33.19	61.9	0.5831	1307	1604
NS	32.45	59.96	0.5349	1300	1551

For the mechanical properties, the compressive strength of the specimens was measured using a Toni Technik compression testing machine (Germany) according to EN 12390-3. The thermal conductivity of the specimens was also evaluated using a Hot Disk, a transient plane source method according to ISO 22007-2. For the mechanical and thermal properties, five to seven tests were carried out in each case to enhance accuracy, and only the average values are presented here.

3.3 Numerical simulation

In addition to the experiments, numerical tests were also performed in pursuit of a more detailed investigation. For the numerical analysis, virtual lightweight concrete specimens were generated, as shown in Fig. 3. The virtual specimens contained the same volume of lightweight aggregates in consideration of the same aggregate grading of the experimental data. The aggregate particles were modeled as spheres since Liaver® has almost an entirely round shape. The sizes of the particles were classified into four classes: 0.5, 1, 2, and 4 mm, allowing for±5% differences in each class. A random packing model of spheres [34] was adopted to describe the LWC specimens with different aggregate sizes. The input parameters for the LWAs and different binders are presented in Table 4; the values in this table were adjusted

from the experimental measurements in Table 2.

The compressive strength and thermal conductivity of the virtual specimens were evaluated using numerical analysis. To compute the properties, a commercial FE package, ABAQUS [35], was used. For the compressive strength, a concrete damaged plasticity (CDP) model in the ABAQUS software was used; this model can be effectively utilized to describe the behavior of quasi-brittle materials by using a scalar damaged factor in the constitutive formulation as follows:

$$\boldsymbol{\sigma} = (1 - d)\boldsymbol{D}^{el} : (\boldsymbol{\epsilon} - \boldsymbol{\epsilon}^{pl}) \tag{1}$$

where $\boldsymbol{\sigma}$ is the stress state function, $\boldsymbol{D}^{el}$ is the initial elastic matrix, $\boldsymbol{\epsilon}$ is the strain tensor, and $\boldsymbol{\epsilon}^{pl}$ is the plastic strain tensor. d is the stiffness degradation variable in the range of 0 (undamaged) and 1 (fully damaged). Detailed formations as well as the required parameters for the simulation can be found in [36, 37, 38]. The number of elements in each virtual specimen was 3,375,000 (150 voxels in x, y, and z directions). Displacement and fixed boundary conditions were applied on the top and bottom surfaces of the specimens, respectively, while the other remaining surfaces were considered to be traction free. The ABAQUS/Explicit solver was employed with an initial time step of 0.01 s, which was found to be enough to ensure the quasi-static loading condition for the mechanical simulations.

Heat flow analysis was also performed using ABAQUS by considering heat loss, and the effective thermal conductivity of the specimens was evaluated in terms of Fourier's law. The required parameters for the heat analysis in Table 4 were given by the manufacturer of Liaver® and measured using the Hot Disk machine. To evaluate the properties of the matrix materials, the specimens only with the binder materials without Liaver® aggregates were produced, and their properties were also measured using the Toni Technik (mechanical) and the Hot Disk (thermal) devices. For the thermal simulation, a constant temperature (60 °C) and a heat loss coefficient (1.4 [1/s]) were assigned on the top and bottom surfaces, respectively. The surrounding temperature was assumed to be 22 °C. The numerical properties were compared with those of the experiments to validate the effects of different binders on material properties.

4 Results and discussions

Pore characteristics are dominant in the mechanical and thermal properties of LWC. Here, μ-CT images were utilized to investigate the pore characteristics of the specimens with different binders. The compressive strength and thermal conductivity of the LWC specimens with different binders are also presented, and the relationship with the pore characteristics is examined.
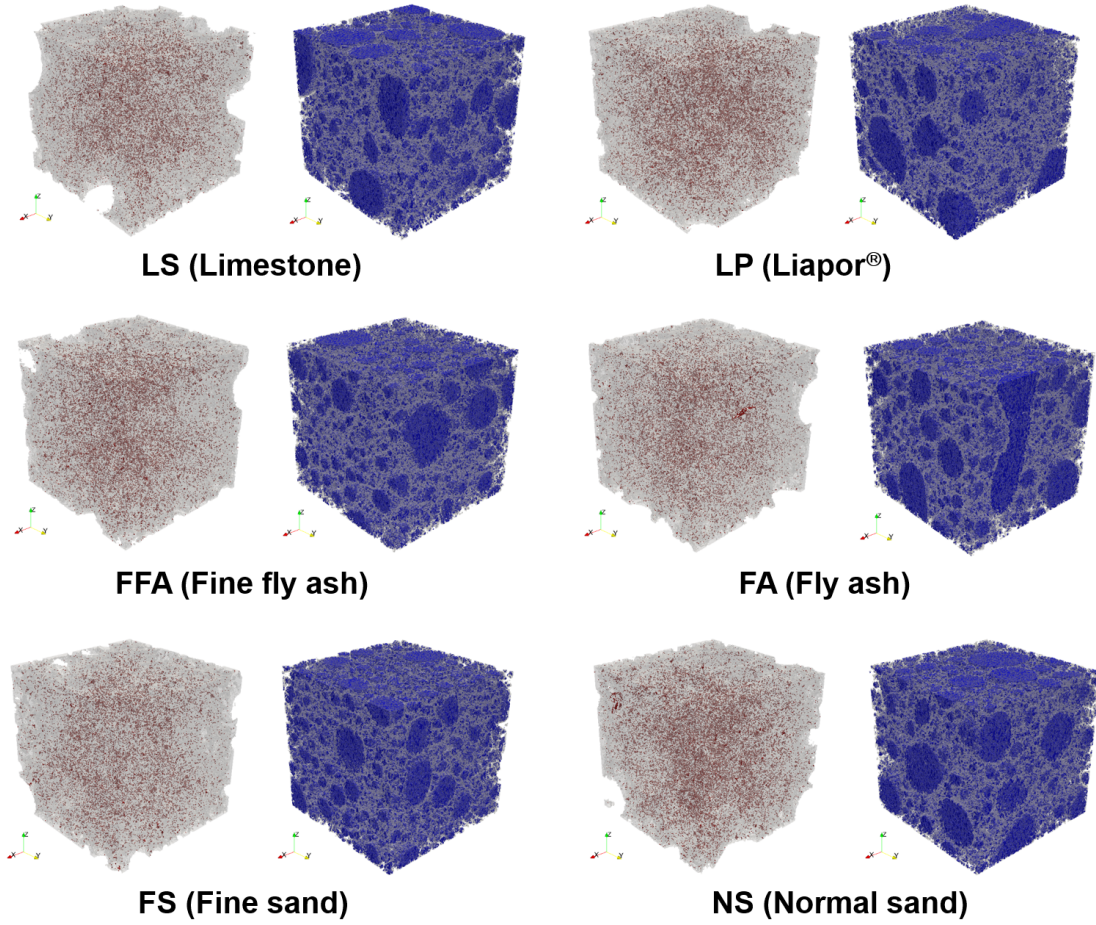
Figure 4: Pore structures of the LWC specimens with different binders (Note: in each specimen, the left figures show the pores in the binder (in red), whilst the right figures present the pores within lightweight aggregates (in blue). In these figures, the light gray phases denote the binder (left) and the aggregate (right) solids.)

4.1 Pore characteristics of the specimens using μ-CT

The pore structures inside the LWC specimens were investigated using μ-CT images. In particular, the pores in the binder and the LWAs were classified using the imaging process so that their effects on the material properties could be evaluated. Fig. 4 presents the pore structures of the LWC specimens with different concrete additions; in this figure, each specimen is categorized into four phases: binder solids, binder pores, aggregate solids, and aggregate pores. As can be seen, all the LWC specimens with different binders are highly porous materials. In particular, a large amount of pores are in existence in the aggregates, while the pores within the binder (in red) are relatively smaller than those within the aggregates (in blue).

Quantitative porosity characterization can be found in Fig. 5. In this figure, the porosities of the matrix and the
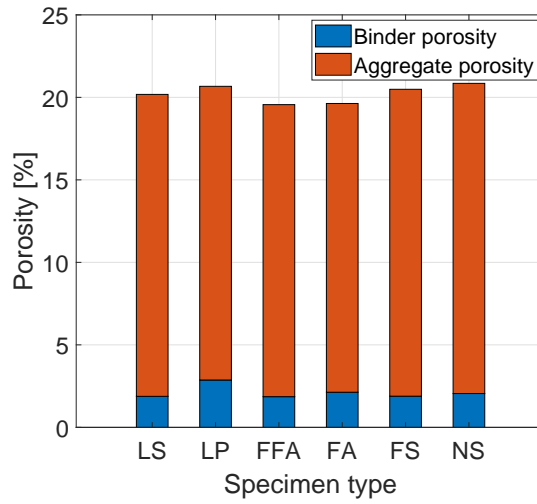
Figure 5: Porosity values of the LWC specimens

aggregates in each specimen, calculated using the μ-CT images, are presented. The pores larger than 29.7 μm were only considered here due to the limited resolution of the μ-CT images. In Fig. 5, the matrix and the aggregate porosities were in the range of 17.6 to 18.8 % and 1.88 to 2.87 %, respectively. As in the pore structure images in Fig. 4, aggregate porosity was dominant in determining material porosity, although binder porosity showed differences according to the binder material. Among the different binders, the LP specimen with Liapor® sand showed the highest porosity, which denotes that this aggregate was the most porous material used in this study. The specimens with fine fly ash (FFA) and normal fly ash (FA) had the lowest porosity, while the LS and FFA specimens contain the lowest matrix porosity. The result in Fig. 5 showed that the LWC specimens with fine/normal fly ash and limestone powder had lower matrix porosity than the other specimens, particularly the specimens with sand. For both fly ash and sand, the specimens with finer materials (FFA and FS) showed lower matrix porosity than those with normal aggregate size; this indicates that finer aggregate can affect the lower porosity of materials by filling pores with small particles. Regarding the porosity, Limestone powder as well as fine materials are more effective in decreasing the porosity of materials, and (fine) fly ash can be considered an appropriate material for producing LWC with low porosity.

In addition to porosity, the solid characteristics of the matrices were investigated using μ-CT images. Fig. 6 shows gray level histograms of the solid phases in each specimen. In this figure, each specimen has different histograms and mean values. Since a gray level μ-CT histogram is strongly related to the density of the material [39, 40], the relative hardness of the matrix can be evaluated using this histogram. In general, a specimen with a higher mean value of the histogram indicates higher density when considering a comparable X-ray attenuation of the present phases. In Fig. 6, the LS specimen has the highest mean value of the binder histogram (67.23), while the mean value of the LP
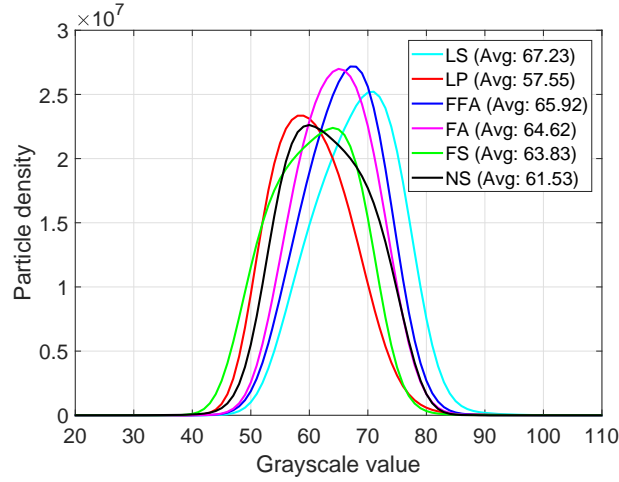
Figure 6: Histogram of the pixel values of the binders in each specimen

specimen is the lowest at 57.55; it represents that the LS specimen contained the most dense solid structure among the specimens, regardless of the porosity of the matrix. The specimens with fine/normal fly ash (FFA/FA) had a higher solid density than the FS and NS specimens. As in the case of the porosity characterization, the specimens with finer aggregates (FFA and FS) showed higher solid densities than those of normal aggregate sizes. The detailed correlation between the pore/solid characteristics and the materials properties will be discussed in the following section.

4.2 Physical properties measured using experimental and numerical approaches

The uniaxial compressive strength of the LWC specimens was evaluated experimentally and numerically. Fig. 7 shows compressive strength, which were measured using the sensitive loading machine (Toni Tecknik) and the FE analysis software (ABAQUS) incorporating the CDP model. In Fig. 7, the average values for five to seven tests of each case are presented as the experimental data. In this figure, the numerical compressive strength values were relatively larger than those found in the experiments. The differences were caused mainly by the pore characteristics of the real specimens and the complexity of the aggregate shapes; the virtual LWC specimens were assumed to have spherical aggregates, while the aggregates included in the real specimens were not complete spheres. In addition, the complex pore structures of the aggregates and minute pores in the binder were not taken into account in the virtual specimens, and homogeneous of the aggregate distribution can result in lower strength of the experimental results. Nevertheless, the differences between the experiments and the simulations are within 14%, which can be considered a reasonable range, and the general trend of the relative magnitude of the compressive strength is the same for both experimental and numerical results.

Among the specimens, the FFA specimen showed the highest compressive strength, while the LP specimen had
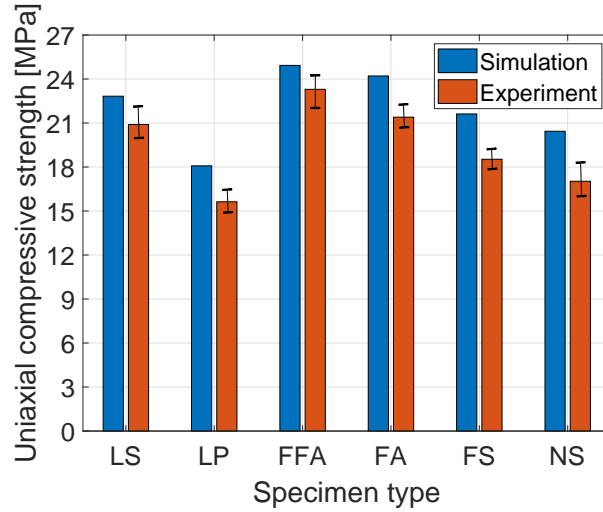
Figure 7: Compressive strength of the LWC specimens measured from the experiment and the simulation

the lowest. The FFA and FA specimens presented better mechanical performance than the FS and NS specimens, and it demonstrates that fly ash is more suitable for LWC with better compressive strength. The LS specimen with limestone powder also showed higher compressive strength than the specimens with fine/normal sand. Comparing the LS and FFA specimens, the FFA specimen showed higher strength than the LS specimen, although the LS specimen had a higher density of the solid phase (Fig. 6) but a higher porosity (Fig. 5); this indicates that the porosity of the material has more of an effect on compressive strength than on density. With the same binder materials, the specimens with finer aggregates (FFA and FS) had higher compressive strengths than that of normal aggregates (FA and NS), because the finer aggregates tended to fill the binder pores and reduce the porosity of the specimens, as shown in Fig. 5. According to these results, when considering only compressive strength, the LWC specimens with fine/normal fly ash were the most effective, whilst Liapor® sand seems to be an ineffective material for producing high-strength lightweight concrete.

However, the compressive strength of materials is determined by several factors, such as porosity, solid structure, and density. Therefore, a more detailed investigation of the mechanical performance of LWC is needed to investigate the effectiveness of different additions. In this study, an efficiency factor [41] was adopted to describe the relationship between density and compressive strength. This is a factor adopted to describe the relationship between the density and compressive strength. Most of lightweight concrete characteristics such as strength and thermal insulation are correlated directly to its dry density. Generally, as the density increases the compressive strength increases. However, in order to compare the experimental results of lightweight concrete mixes with different composition, it is difficult to compare both density as well as strength at the same time. Therefore, it is important to find a method to compare
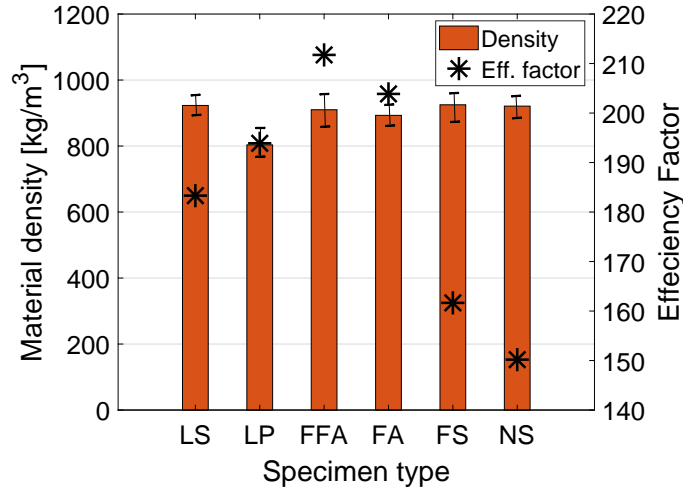
Figure 8: Material density and efficiency factor of the LWC specimens

the performance of lightweight concrete mixes with different dry densities. The efficiency factor used in this study is a parameter which is determined from the ratio of compressive strength and density of concrete. In general, concrete with an efficiency factor larger than 70 is considered to be acceptable, and the factor can be calculated as follows:

$$F_{eff} = \frac{F_c}{(p/2.2)^{2.5}} \tag{2}$$

where F_c and p are the compressive strength at 28 days and the dry density of the material, respectively.

In Fig. 8, the specimen density and the efficiency factor of each LWC are presented. The figure shows that most of the specimens had similar density values, except for the LP specimen. In particular, the density of the FFA and FA specimens was slightly lower than that of the LS, FS, and NS specimens, with their efficiency factors having been much higher than those of the other specimens since the compressive strength of the FFA and FA specimens was higher than that of the other specimens with similar densities. The LP specimen had the lowest density amongst all the cases in this study, due to its porous material characteristics; however, its efficiency factor was higher than that of the LS, FS, and NS specimens, which indicates that Liapor® sand is an effective material regarding density and compressive strength, even though the LP specimen had the lowest density and compressive strength. The results in Fig. 8 confirm that LWC with fine fly ash filler showed the best mechanical performance amongst the cases used here in regard to compressive strength and efficiency factor.

The thermal conductivity of the LWC specimens was also evaluated using both experimental and numerical approaches. Fig. 9 presents the effective thermal conductivity values of the specimens. As with compressive strength, the
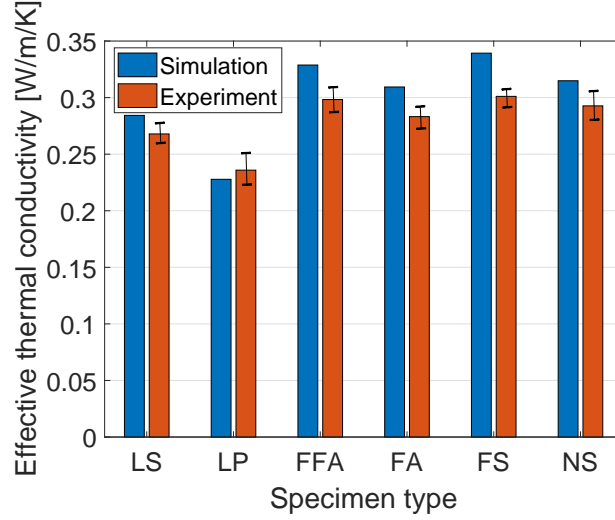
Figure 9: Thermal conductivity of the LWC specimens measured from the experiment and the simulation

relative size and thermal conductivity trends measured by both methods are similar; the maximum difference between the experimental and the numerical data is about 11%. In general, the specimens with higher compressive strength tended to show higher thermal conductivity. Among the samples, the LP specimen had the lowest thermal conductivity due to its high porosity and relatively sparse solids and can be effectively used to enhance the insulation of the material. The specimens with fine/normal sand had the highest thermal conductivity, even though their porosities were higher than that of the other specimens; it can be inferred that the matrix made from sand is composed of constituents with higher thermal conductivity. In addition, the specimens with finer aggregates presented higher thermal conductivity than the specimens with normal aggregates due to their dense solid structures. The results demonstrate that the general trend of thermal conductivity is more comparable to the porosity of the specimens, rather than their solid phase characteristics. Since the mechanical and thermal properties of the specimens with different binders are contrary, it should be noted that the concrete additions for LWC needs to be selected according to the purpose of use.

5 Conclusions

This study has demonstrated the effects of different concrete additions on the behavior of lightweight aggregate concrete. Six materials, limestone powder, Liapor® sand, fine/normal fly ash, and fine/normal sand, were used as concrete additions, and lightweight concrete specimens with the same lightweight aggregate (Liaver®) but different concrete additions were produced. Virtual lightweight specimens were also generated to clarify the effect of the binder types. Experiments and numerical simulations incorporating μ-CT images were utilized to characterize and evaluate the

material properties of the specimens.

The concluding remarks of this study are as follows:

- Lightweight aggregate concrete with a density less than 1000 kg/m^3 was produced by using expanded lightweight aggregates and different concrete additions. All specimens produced in this study had a compressive strength of more than 18 MPa and a thermal conductivity of less than 0.35 W/m/K, meaning they could be utilized as high-performance lightweight concrete.

- Virtual lightweight specimens, which took into account the experimental conditions, were generated and used to verify the effects of the binders. The numerical results confirmed that virtual specimens can be used to predict and demonstrate the performance of real lightweight concrete.

- X-ray μ-CT images can be effectively used to visualize the pore structures of lightweight aggregate concrete. In particular, the pores in the matrix and aggregates were classified and characterized using the μ-CT images.

- Considering the compressive strength of the materials, fine/normal fly ash gave the best mechanical properties amongst the cases examined in this study. In particular, binders with finer materials showed a higher compressive strength than normal ones. On the other hand, materials with porous structures as well as sparse solids show lower thermal conductivity, which is beneficial for better insulation. On the whole, among the specimens used here, the LS specimen with limestone powder most effectively satisfies both thermal and mechanical properties because of its low thermal conductivity as well as its relatively high compressive strength.

- Both pore and solid characteristics should be carefully considered to produce a material which satisfies the purpose of use.

In addition to the results of this study, the systematic investigation tools used here can be utilized for further development of advanced lightweight concrete as well as for special building materials with particular objectives.

Acknowledgements

References

[1] A. M. Neville, Properties of concrete, Wiley, Chichester, 2012.

[2] S. Mindess, J. F. Young, D. Darwin, Concrete, 2nd Ed., Prentice Hall, New York, 2002.

[3] N. Narayanan, K. Ramamurthy, Structure and properties of aerated concrete: a review, Cement and Concrete Composites 22 (2000) 321–329.

[4] M. Aslam, P. Shafigh, M. Z. Jumaat, Oil-palm by-products as lightweight aggregate in concrete mixture: a review, Journal of Cleaner Production 126 (2016) 56–73.

[5] F. Roberz, R. C. G. M. Loonen, P. Hoes, J. L. M. Hensen, Ultra-lightweight concrete: Energy and comfort performance evaluation in relation to buildings with low and high thermal mass, Energy and Buildings 138 (2017) 432–442.

[6] S.-Y. Chung, M. A. Elrahman, P. Sikora, T. Rucinska, E. Horszczaruk, D. Stephan, Evaluation of the effects of crushed and expanded waste glass aggregates on the material properties of lightweight concrete using image-based approaches, Materials 10 (2017) 1354.

[7] C. Muoz-Ruiperez, A. Rodrguez, S. Gutirrez-Gonzlez, V. Caldern, Lightweight masonry mortars made with expanded clay and recycled aggregates, Construction and Building Materials 118 (2016) 139–145.

[8] S.-Y. Chung, M. A. Elrahman, D. Stephan, Effect of different gradings of lightweight aggregates on the properties of concrete, Applied Sciences 7 (2017) 585:1–15.

[9] A. Mueller, A. Schnell, K. Ruebner, The manufacture of lightweight aggregates from recycled masonry rubble, Construction and Building Materials 98 (2015) 376–387.

[10] P. Sikora, A. Augustyniak, K. Cendrowski, E. Horszczaruk, T. Rucinska, P. Nawrotek, E. Mijowska, Characterization of mechanical and bactericidal properties of cement mortars containing waste glass aggregate and nanomaterials, Materials 9 (2016) 701.

[11] H. J. H. Brouwers, H. J. Radix, Self compacting concrete: theoretical and experimental study, Cement and Concrete Research 35 (2005) 2116–2136.

[12] T. Y. Lo, W. C. Tang, H. Z. Cui, The effects of aggregate properties on lightweight concrete, Building and Environment 42 (2007) 3025–3029.

[13] R. Yu, D. V. van Onna, P. Spiesz, Q. L. Yu, H. J. H. Brouwers, Development of ultra-lightweight fibre reinforced concrete applying expanded waste glass, Journal of Cleaner Production 112 (2016) 690–701.

[14] I. Lukic, M. Malesev, V. Radonjanin, V. Bulatovic, Basic properties of structural LWAC based on waste and recycled materials, Journal of Materials in Civil Engineering 29 (2017) 1–5.

[15] P. K. Mehta, P. J. M. Monteiro, Concrete: microstructure, properties and materials, 4th Ed., McGraw-Hill, New York, 2015.

[16] J. M. Paris, J. G. Roessler, C. C. Ferraro, H. D. DeFord, T. G. Townsend, A review of waste produces utilized as supplements to portland cement in concrete, Journal of Cleaner Production 121 (2016) 1–18.

[17] Z. Zhang, Q. Wang, H. Chen, Y. Zhou, Influence of the initial moist curing time on the sulfate attack resistance of concretes with different binders, Construction and Building Materials 144 (2017) 541–551.

[18] Y. Diquelou, E. Gourlay, L. Arnaud, B. Kurek, Influence of binder characteristics on the setting and hardening of hemp lightweight concrete, Construction and Building Materials 112 (2016) 506–517.

[19] S. Real, J. A. Bogas, Oxygen permeability of structural lightweight aggrgate concrete, Construction and Building Materials 137 (2017) 21–34.

[20] S. Real, J. A. Bogas, J. Pontes, Chloride migration in structural lightweight aggregate concrete produced with different binders, Construction and Building Materials 98 (2015) 425–436.

[21] T. C. Fu, W. Yeih, J. J. Chang, R. Huang, The influence of aggregate size and binder material on the properties of pervious concrete, Advanced in Materials Science and Engieering 963971 (2014) 1–17.

[22] P. Shafigh, M. A. Nomeli, U. J. Alengaram, H. B. Mahmud, M. Z. Jumaat, Engineering properties of lightweight aggregate concrete containing limestone powder and high volume fly ash, Journal of Cleaner Production 135 (2016) 148–157.

[23] K. H. Mo, T.-C. Ling, U. J. Alengaram, S. P. Yap, C. W. Yuen, Overview of supplementary cementitious materials usage in lightweight aggregate concrete, Construction and Building Materials 139 (2017) 403–418.

[24] J. N. Farahani, P. Shafigh, B. Alsubari, S. Shahnazar, H. B. Mahmud, Engineering properties of lightweight aggregate concrete containing binary and ternary blended cement, Journal of Cleaner Production 149 (2017) 976–988.

[25] ECS, Concrete - Part 1: Specification, performance, production and conformity, EN 206-1:2000, Brussels, Belgium, 2000.

[26] EN 12390-4:2000, Testing hardened concrete–Part 4: Compressive strength; specification for testing machines (Jul. 2000).

[27] ISO 22007-2:2015, Plastics–determination of thermal conductivity and thermal diffusivity–part 2: Transient plane heat source (Hot Disk) method (Aug. 2015).

[28] EuroLightCon, LWAC material properties state–of–the–art. In:Economic design and construction with light weight aggregate concrete, Brite-EuRam III, 1998.

[29] ECS, Tests for mechanical and physical properties of aggregates. Determination of particle density and water absorption, EN 1097-6:2013, Brussels, Belgium, 2013.

[30] A. Andreasen, J. Andersen, Über die Beziehungen zwischen Kornabstufungen und Zwischenraum in Produkten aus losen Körnern (in German), Kolloid-Zeitschrif 50 (1930) 217–228.

[31] H. J. H. Brouwers, Particle-size distribution and packing fraction of geometric random packings, Physical Review E 74 (2006) 031309.

[32] D.-Y. Huang, C.-H. Wang, Optimal multi-level thresholding using a two-stage otsu optimization approach, Pattern Recognition Letters 30 (2009) 275–284.

[33] S.-Y. Chung, C. Lehmann, M. A. Elrahman, D. Stephan, Pore characteristics and their effects on the material properties of foamed concrete evaluated using micro-ct images and numerical approaches, Applied Sciences 7 (2017) 550:1–19.

[34] K. Sobolev, A. Amirjanov, Application of genetic algorithm for modeling of dense packing of concrete aggergates, Construction and Building Materials 24 (2010) 1449–1455.

[35] ABAQUS, Version 6.13, Dassault Systemes, Pawtucket, Rhode Island, 2013.

[36] M. Bolhassani, A. A. Hamid, A. C. W. Lau, F. Moon, Simplified micro modeling of partially grouted masonry assemblages, Construction and Building Materials 83 (2015) 159–173.

[37] M. R. Jones, Foamed concrete for structural use. In: Proceeding of one day seminar on foamed concrete: properties, applications and latest technological developments, Loughborough University, 2001.

[38] P. Kmiecik, M. Kaminski, Modelling of reinforced concrete structures and composite structures with concrete strength degradation taken into consideration, Archives of Civil and Mechanical Engineering 11 (2011) 623–636.

[39] D. Gastaldi, F. Canonico, L. Capelli, E. Boccaleri, M. Milanesio, L. Palin, G. Croce, F. Marone, K. Mader, M. Stampanoni, In situ tomographic investigation on the early hydration behaviors of cementing systems, Construction and Building Materials 29 (2012) 284–290.

[40] H. Lu, E. Alymov, S. Shah, K. Peterson, Measurement of air void system in lightweight concrete by X-ray computed tomography, Construction and Building Materials 152 (2017) 467–483.

[41] A. Hueckler, Trag- und Verformungsverhalten von biegebeanspruchten Bauteilen aus Infraleichtbeton (ILC) (German), Sierke Verlag, Germany, 2016.